COBEM 2021 26th International Congress of Mechanical Engineering
November 22-26, 2021, Virtual Congress, Brazil
ABCM Associação Brasileira de Engenharia e Ciências Mecânicas

COB-2021-0497
DEVELOPMENT AND COMPARISON OF PLANAR AND CONICAL SCRAMJET VEHICLE INLET

Luiz Henrique Silva Marques Soares
Instituto Tecnológico de Aeronáutica/ITA, Praça Marechal Eduardo Gomes, 50 - Vila das Acacias, CEP 12228-900, São José dos Campos/SP, Brazil
luizlhsms@ita.br

Heidi Korzenowski
Universidade do Vale do Paraíba/UNIVAP - Faculdade de Engenharias, Arquitetura e Urbanismo - Av. Shishima Hifumi nº 2911, Urbanova, CEP 12.224-000, São José dos Campos/SP, Brazil
heidi.korzenowski@gmail.com

Paulo Gilberto de Paula Toro
Universidade Federal do Rio Grande do Norte/UFRN - Centro de Tecnologia. Av. Senador Salgado Filho, 3000 - Campus Universitário, Lagoa Nova, CEP 59.078-970 – Natal/RN - Brazil
toro11pt@gmail.com

João Felipe de Araújo Martos
Universidade Federal de Santa Maria/UFSM - Centro de Tecnologia. Av. Roraima, 1000 - Cidade Universitária, Camobi, CEP 97105-900 – Santa Maria/RS - Brazil
joao.martos@ufsm.br

Abstract. *This work presents the development and comparison of planar and conical configurations for the compression section of a hypersonic airbreathing vehicle, using scramjet technology. The analysis of different configurations in the initial stages of the design of scramjet vehicles is necessary to determine the most suitable one to be applied based on the requirements of the project. Thus, the evaluation of the planar and conical inlets was considered to compare the influence of the choice of configuration on the performance and dimensions of the scramjet vehicles inlet. In order to perform a conservative analysis, the hypothesis of perfect gas and inviscid flow was considered, applying the theoretical-analytical and numerical analyzes, respectively, for each configuration. For the planar inlet, the theory of planar oblique shock waves was applied. As for the conical inlet, the theory of conical oblique shock waves was applied using the Taylor-Maccoll solution with the necessary adaptations for application in more than one subsequent cone. In order to optimize geometries and minimize performance losses during compression, the maximum pressure recovery method was applied. Subsequently, a case study was proposed considering the Mach number 7 and 30 km of geometric altitude, of which a model for each configuration was developed. Then, it was evaluated in computational fluid dynamic (CFD) simulations using the ANSYS - Fluent 19.2 code in order to compare with the analytical results. In the end, it was verified the applicability of the formulation for the definition of scramjet vehicles inlet, with the convergence between the analytical and numerical results. Subsequently, the results obtained were presented in a comparative manner, highlighting the dimensional and performance differences that the variation in geometry causes. Thus, the importance of evaluating the different geometries that can be applied in the scramjet inlets was emphasized.*

Keywords: *Hypersonic, Airbreathing Propulsion, Scramjet, Oblique Shock Wave, Conical Shock Wave.*

1. INTRODUCTION

According to Pezzella and Viviani (2019), the growth of manned or unmanned space missions, in Low Earth Orbit, LEO, demands an evolution in cargo transport vehicles linked to flexibility, accessibility, and safety in routine access to space. Thus, motivated by space exploration and fast mobility, hypersonic technology has been gaining scope in the academic and industrial context. The use of hypersonic airbreathing vehicles, combined with traditional rocket engines, will enable a significant increase in the efficiency of launcher vehicles since airbreathing vehicles use atmospheric air as an oxidizer.

In the 1950s, conventional ramjet engines, designed to operate in flight range in Mach number 3 to 6 and fueled by

hydrocarbons, were under constant development due to their diverse applications in high-speed missiles. However, according to Curran (2001), when the flight Mach number exceeds 6, decelerating the flow to the subsonic regime generates very high pressures and temperatures in the combustion chamber, in some cases, above that supported by the structure.

To develop aircraft and missiles with even higher operating speeds, there was a wide range of research based on the ramjet engine with supersonic combustion, scramjet, with its main attraction being the operating speed because it performs combustion in a supersonic flow (Curran, 2001).

In this way, from one or more oblique shock waves, the supersonic flow is partially compressed. Considering energy conservation, part of the kinetic energy of the flow is transformed into internal energy and, thus, it results in increases in temperature, pressure, and density of the air, as well as a decrease in the flow velocity, remaining in a supersonic regime, to provide a flow with adequate thermodynamic conditions for fuel ignition.

According to Curran and Murthy (2000), in the compression section of hypersonic airbreathing vehicles, different geometries are developed in an attempt to provide high performance without violating design constraints. The choice for a given geometry is the result of compensating analyzes between performance, weight, production capacity, for example. In this way, different configurations can be used to meet design requirements such as Planar, Oswatitisch, Busemann, REST, among others.

Planar geometry, Figure 1, uses a series of plane ramps that aim to perform a partial compression of the flow from the formation of plane oblique shock waves. The ramps are developed, normally from the analytical relations of oblique shock waves, to guarantee the efficient compression and high performance of the vehicle. In general, the waves affect the cowl to form a reflected shock wave that aligns the flow to enter parallel and uniformly into the combustion chamber.

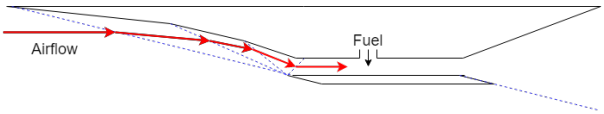

Figure 1: Schematic of supersonic planar inlet.

Oswatitisch geometry, illustrated in Figure 2, consists of a compression based on the formation of conical oblique shock waves linked to a single reflection in the cowl. The geometry can be developed from the Method of Characteristics or from the solution of the hypersonic flow passing through a cone, as presented by the Taylor-Maccoll solution. The reflected shock wave is responsible for linearizing the flow so that a uniform and parallel flow is provided to the combustion chamber.

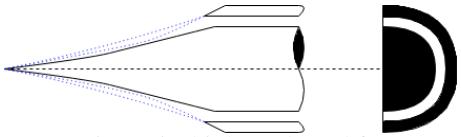

Figure 2: Schematic of supersonic conical inlet (adapted from Curran and Murthy (2000)).

During the preliminary design of aerospace systems, it is common to survey needs, define requirements and subsequently generate initial configurations that can be comparatively evaluated and the results can be used as justification for choosing a particular configuration.

In this context, the motivation is the study and implementation of quick, simplified, and concise methodologies about the development of compression sections (inlets) of hypersonic airbreathing vehicles using, as a basis, planar and Oswatitisch (conical) geometries.

2. METHODOLOGY

Initially, it is necessary to describe the nomenclature to be used in scramjet vehicles. Since planar and conical geometries have slightly similar geometric configurations, it is possible to use the same general nomenclature, Figure 3.

Subdivided according to Figure 3, the compression section (1-3), is responsible for performing the flow compression for a flow with the desired temperature, pressure, and density at the entrance of the combustor, maintaining the supersonic velocity conditions. The external compression section (1-2) is governed by the formation of plane oblique shock waves for the planar geometry and the formation of conical oblique shock waves for the conical geometry. The internal compression section (2-3) is governed by the formation of oblique reflected shock waves and is responsible for providing a uniform and parallel flow at the entrance to the combustor.

Therefore, to obtain optimized inlets, the design by total pressure recovery inlet theory proposed by Ran and Mavris (2005) for the planar configuration is considered and adaptations are performed to consider the same theory for the conical configuration.

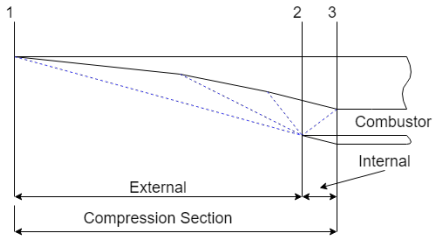

Figure 3: Schematic of supersonic inlet (adapted from Heiser and Pratt (1994)).

2.1 Shock wave theory

According to Anderson (2003), when an object moves through a gas, the molecules are shifted around the object. If the object's velocity is much lower than the velocity of sound, the density of the gas remains constant and the flow can be described considering the conservation of momentum, mass, and energy. However, when the speed of the object approaches the speed of sound, compressibility effects start to appear with the variation of the local density of the gas as it is compressed by the object.

For compressible flows with small directional change, the reversible process with constant entropy is considered. However, as mentioned by Martos (2017), when objects move at a speed above the speed of sound in the environment, there is a considerable change in the flow direction and shock waves are generated. These waves are small regions where the velocity and thermodynamic properties of the flow such as temperature, density, and pressure change almost instantaneously so that the process is not isentropic.

2.1.1 Plane oblique shock wave theory

According to Anderson (2003), plane oblique shocks usually occur when a supersonic or hypersonic flow presents a positive direction variation in relation to the plane resulting from the deflection of a surface in a θ angle, Figure 4.

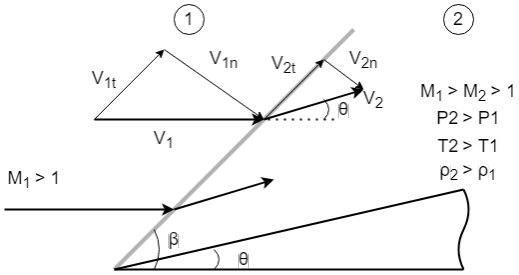

Figure 4: Plane oblique shock wave analysis.

From the Navier-Stokes system of equations, presented in Anderson (2003), and considering the simplifications of one-dimensional flow, Stationary flow, adiabatic flow, Inviscid flow, disregarding body forces, and considering a calorically perfect gas, the Continuity, Momentum, and Energy equations are obtained. From them and the geometric analysis of Figure 4, considering V_1 and V_2 the flow velocities in 1 and 2 regions and V_{1t}, V_{1n},V_{2t}, V_{2n} the tangential and normal components of the V_1 and V_2 it is possible to obtain the $\theta - \beta - M$ relations between the surface angle θ and the angle of the plane oblique shock wave β, the normal Mach number before the plane oblique shock wave, and the ratios between density, pressure and temperature and the normal and total Mach number after the plane oblique shock wave, respectively.

$$\tan\theta = 2\cot\beta\left[\frac{M_1^2\sin^2\beta - 1}{M_1^2(\gamma + \cos 2\beta) + 2}\right]. \tag{1}$$

$$M_{1_n} = M_1 sen\beta; \tag{2}$$

$$\frac{\rho_2}{\rho_1} = \frac{(\gamma+1)M_{n_1}^2}{(\gamma-1)M_{n_1}^2 + 2}; \tag{3}$$

$$\frac{T_2}{T_1} = \frac{p_2}{p_1}\frac{\rho_1}{\rho_2}; \tag{4}$$

$$\frac{p_2}{p_1} = 1 + \frac{2\gamma}{\gamma+1}\left(M_{n_1}^2 - 1\right); \tag{5}$$

$$M_{n_2}^2 = \frac{M_{n_1}^2 + [2/(\gamma-1)]}{[2\gamma/(\gamma-1)]M_{n_1}^2 - 1}; \tag{6}$$

$$M_2 = \frac{M_{n_2}}{\sin(\beta-\theta)}; \tag{7}$$

Across the shock wave, the Mach number reduce, maintaining the supersonic regime, and pressure, temperature, and density increase.

2.1.2 Conical oblique shock wave

According to Anderson (2003), conical oblique shocks are plane oblique shocks formed by a supersonic flow incident on a conical geometry. The thermodynamic properties of the flow after the conical shock wave are calculated with relationships similar to oblique shock waves. However, unlike the plane oblique shock wave, because the flow around a cone is three-dimensional, the flow after the conic shock wave is not uniform, Figure 5. The flow lines are curved and the flow properties in the cone surface P_c are different from the resulting properties after the conical shock wave P_2.

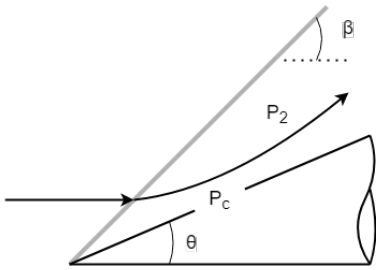

Figure 5: Supersonic flow incident on conical geometry (adapted from Anderson (2003)).

According to Anderson (2003), the three-dimensional supersonic flow incident on a cone is considered axisymmetric and has an exact non-linear solution solved from a numerical integral.

Starting from the system of Navier-Stokes equations in spherical coordinates and considering the one-dimensional, stationary, adiabatic, inviscid flow and considering the calorically perfect gas, as presented by Anderson (2003), it finds the Taylor-Maccoll Equation, Equation 8, which is an ordinary differential equation that presents the solution for conical flows and is dependent on the velocity variables in the direction r e θ.

$$\frac{\gamma-1}{2}\left[1 - {\mathrm{V_r}}^2 - \left(\frac{\mathrm{dV_r}}{\mathrm{d}\theta}\right)^2\right]\left[2\mathrm{V_r} + \cot\theta\frac{\mathrm{dV_r}}{\mathrm{d}\theta} + \frac{\mathrm{d^2V_r}}{\mathrm{d}\theta^2}\right] - \frac{\mathrm{dV_r}}{\mathrm{d}\theta}\left[\mathrm{V_r}\frac{\mathrm{dV_r}}{\mathrm{d}\theta} + \frac{\mathrm{dV_r}}{\mathrm{d}\theta}\frac{\mathrm{d^2V_r}}{\mathrm{d}\theta^2}\right] = 0, \tag{8}$$

$$V_\theta = \frac{dV_r}{d\theta}. \tag{9}$$

2.2 Total pressure recovery theory

Ran and Mavris (2005), suggest a methodology that uses an optimization criterion to determine the angle of the ramps in a supersonic compression section for total pressure recovery. According to the authors, the loss of total pressure directly influences the decrease in thrust and, consequently, the increase in fuel consumption. Methodology initially proposed by Oswatitsch (1947) and applied to the hypersonic scramjet inlet by Martos (2017) suggests that in a system with n-1 incident oblique shock waves, Figure 6, the total pressure recovery is achieved when the waves oblique shock waves have the same intensity, that is, when the normal velocity component of the shock wave is equal in all incident waves.

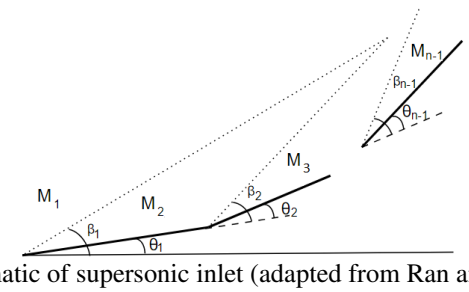

Figure 6: Schematic of supersonic inlet (adapted from Ran and Mavris (2005)).

In this way, the intensity of the shock waves and the total pressure ratio through an oblique shock wave is given, respectively by

$$M_1 sin\beta_1 = M_2 sin\beta_2 = M_{n-1} sin\beta_{n-1}, \tag{10}$$

$$\Pi = \frac{p_{out}}{p_{in}} \left\{ \frac{1 + \frac{\gamma-1}{2} M_{out}^2}{1 + \frac{\gamma-1}{2} M_{in}^2} \right\}^{\gamma/(\gamma-1)} . \tag{11}$$

2.3 Reflected oblique shock wave

According to Anderson (2003), a reflected oblique shock wave occurs when an oblique shock wave incides a solid surface, Figure 7. Similarly, to the incident oblique wave theory, the flow adjusts to the surface boundary conditions, making it if parallel to that. Oblique shock wave theory is used for incident shock waves and also for the reflected shock wave.

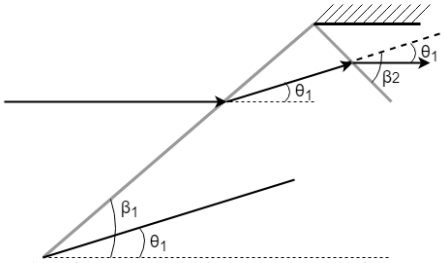

Figure 7: Schematic of supersonic inlet (adapted from Anderson (2003)).

3. SYSTEM MODELING

To provide the modeling of the system with less computational use and more intuitively, you need to break it down into subsystems. As the configurations have different formulations, it is necessary to elaborate computational routines directed to each configuration.

3.1 Planar configuration

According to Figure 8, the routine for the planar configuration was modeled from the design parameters that comprise the definition of dimensional requirements, design requirements, such as the desired properties at the input of the combustor, and flight parameters, such as speed, the altitude and the thermodynamic properties of the freestream flow determined according to Atmosphere (1976). Subsequently, the number of ramps is defined and an estimate is made for the angle of the first ramp. Therefore, from the theory of the plane oblique shock wave, the angle of the first plane oblique shock wave is defined and the thermodynamic properties of the flow after the first shock wave are calculated. Afterward, considering the total pressure recovery theory, the next shock waves are determined and, consequently, the ramps generated them. In the end, the reflected shock wave is calculated and thus the properties at the input of the combustor are determined. If the properties found are different from those desired, increments are made in the angle of the first ramp until the desired thermodynamic properties at the input of the combustor are found.At the end, the length of the ramps is set so that the oblique shock waves insides the leading edge of the cowl (shock on-lip) and the reflected shock wave hits the combustor inlet (shock on-corner).

3.2 Conical configuration

Similar to the plane configuration and according to Figure 9, the routine for the plane configuration was modeled from dimensional requirements, design, and flight parameters. After defining the number of cones and knowing the freestream properties, an initial estimate for the angle of the first cone is performed.

To determine the β responsible for generating the estimated θ, it is necessary to numerically solve the Taylor-Maccoll Equation, Equation 13. In general, the MATLAB software has ODE family integrators that solve functions of type $y(t)$ that satisfy $y_0 = f(t, y)$ calculated from an initial value $y(t_0)$. According to Lassaline (2009), it is convenient to adopt, in this case, a solution vector in which

$$y = \begin{bmatrix} y_1 \\ y_2 \end{bmatrix} = \begin{bmatrix} V_r \\ V_r' \end{bmatrix} = \begin{bmatrix} V_r \\ V_\theta \end{bmatrix}. \tag{12}$$

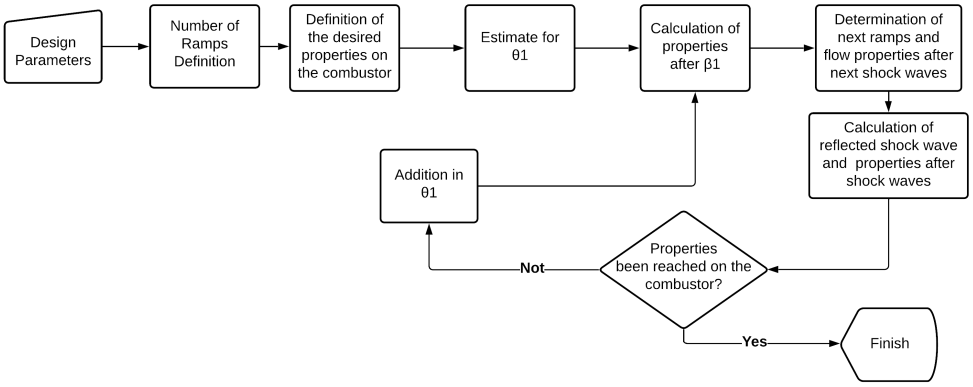

Figure 8: Schematic of scramjet planar inlet methodology.

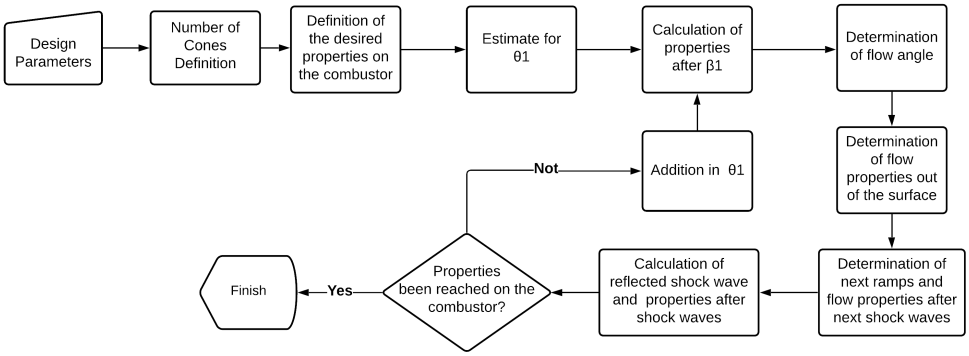

Figure 9: Schematic of scramjet conical inlet methodology..

Thus, it is necessary to write the Taylor-Maccoll Equation in the differential form $y_0 = f(\theta, y)$

$$y' = f(\theta, y) = \begin{bmatrix} y_2 \\ \frac{y_2^2 y_1 - \frac{\gamma-1}{2}\left(1-y_1^2-y_2^2\right)(2y_1+y_2\cot(\theta))}{\frac{\gamma-1}{2}\left(1-y_1^2-y_2^2\right)-y_2^2} \end{bmatrix}. \tag{13}$$

To properly compute an initial value for the solution, it is estimated that the initial value of β is the angle formed by an equivalent plane oblique shock wave, β_s, Figure 10.

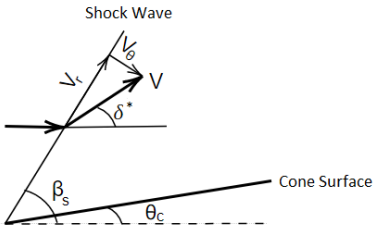

Figure 10: Supersonic flow on conical surface (adapted from Lassaline (2009)).

The method consists of solving Equation 13 numerically, starting from β_s, until finding the θ_c, which makes the variable $y_2 = 0$. That is when evaluating the flow on the cone surface, $V_\theta = 0$ and, therefore, $y_2 = 0$.

The Mach number on the cone surface after the conical oblique shock wave is defined by the tangential component that meets the numerical solution obtained. Furthermore, the flow properties after shocks are obtained from the plane oblique shock waves theory. The Mach number out the cone surface is defined considering the plane oblique shock wave relationships.

Due to the presence of several cones, it is necessary to consider the flow angle, δ^*, to compute the correct incidence of the angle in the next cone. The angle of flow after the conical shock can be approximated to the surface angle θ of the $\theta - \beta - M$ relation for the plane oblique shock wave. Similar to the routine adopted for the planar configuration, the intensity of the first shock wave is defined, that is, the velocity normal to the wave, and it is adopted that the other waves have the same intensity. Finally, knowing the properties of the flow along with the shock waves, the reflection in the cowl

is calculated and, later, the characteristics of the flow at the entrance of the combustor are defined. Similarly, the length of the ramps is set to result in shock on-lip and shock on-corner.

4. RESULTS AND COMMENTARIES

4.1 Analytical Results

To carry out a comparative analysis between the two configurations, similar design parameters were defined: Flight at 30 km of geometric altitude, at Mach number 7 and both coupled to the same rocket engine to ensure the same dimensional restrictions.

Initially, it is necessary to determine the thermodynamic properties of the air at 30 km of geometric altitude, Table 1.

Table 1: Thermodynamic atmospheric properties at 30 km altitude (Atmosphere, 1976).

Geometric Altitude (Z) [km]	**Temperature (T)** [K]	**Pressure (p) [Pa]**	**Density (ρ) [kg/m³]**	**Speed of Sound (a) [m/s]**
30	226.5	1197	0.01841	301.7

Afterward, it is necessary to define the dimensional requirements. Considering the cross section of the rocket engine described by Pereira (2018), it is necessary to consider how each configuration is coupled to the rocket engine, Figure 11.

(a) Planar scramjet on rocket engine. (b) Conical scramjet on rocket engine.

Figure 11: Scramjet vehicles coupled at the rocket engine.

The conical configuration visually is better suited to the configuration of the rocket, making better use of the available area. This fact is also demonstrated when calculating mass flow flux at the front of vehicles: For the planar configuration, the flow mass flux at the inlet is 1.3073 kg/m^3. For the conical configuration, it is 4.4095 kg/m^3.

Later, in defining the number of ramps, Martos (2017) analyzes the relationship between the number of ramps and compression efficiency and determines that three ramps are the optimal point between efficiency and complexity considering the methodology of total pressure recovery and effects of manufacturing complexity. Similarly, considering the data presented by Martos (2017) as a reference, the necessary temperature of 1100 K at the entrance of the combustor was estimated.

From the definition of the methodology and design parameters, it is possible to define the geometric results obtained from the planar and conical configurations.

Table 2: Planar scramjet vehicle geometric results.

Planar configuration					
	Ramp 1	**Ramp 2**	**Ramp 3**	**Reflection (Combustor)**	**Total**
θ	6.124º	7.238º	8.609º	21.971º	-
β	12.777º	15.186º	18.218º	34.399º	-
Length	0.486 m	0.216 m	0.206 m	(0.0822 m)	0.9685

Furthermore, the results of the thermodynamic properties of the flow along the inlets are obtained. For the thermodynamic properties of the conic configuration, the items with subscript c refer to the properties on the surface of the cones.

It is verified that the flow temperature criterion above 1100 K at the entrance of the combustion chamber with the supersonic flow was reached. It is observed that the flow in the conical configuration has an approximate angle different from the angle of the cone, highlighting the need to consider the direction of flow in the methodology. Furthermore, due to the three-dimensional effect of the problem, to result in the same thermodynamic conditions, compared with the planar

Table 3: Conical scramjet vehicle geometric results.

Conical configuration					
	Ramp 1	**Ramp 2**	**Ramp 3**	**Reflection (Combustor)**	**Total**
$\theta_{Calculated}$	8.379º	9.706º	11.304º	29.391º	-
δ^*	3.0410º	3.5381º	4.147º	-	-
θ_{Real}	8.990º	6.665º	7.766º	23.775º	-
β	12.107º	14.051º	16.414º	35.582º	-
Length	0.6615 m	0.130 m	0.1227 m	(0.0822 m)	0.9965

Table 4: Results of thermodynamic properties along planar vehicle.

	M [-]	**p [Pa]**	**T [K]**	ρ**[kg/m^3]**	**a [m/s]**
Freestream	7	1197	226.5	0.01841	301.7
Ramp 1	5.909	3147.510	306.358	0.0357	350.848
Ramp 2	4.951	8276.375	414.356	0.0695	408.030
Ramp 3	4.101	21762.723	560.426	0.1352	474.530
Combustor Entrance	2.473	132722.114	1100.001	0.4203	664.816

Table 5: Results of thermodynamic properties along conical vehicle.

	M (M_c)**[-]**	**p** (p_c)**[Pa]**	**T**(T_c)**[K]**	$\rho(\rho_c)$**[kg/m^3]**	**a**(a_c)**[m/s]**
Freestream	7	1197	226.5	0.01841	301.7
Ramp 1	6.046 (5.896)	2810.789 (3280.165)	294.270 (307.545)	0.0332 (0.0378)	301.680 (351.527)
Ramp 2	5.195 (5.0610)	6600.280 (17535.783)	382.303 (399.549)	0.0601 (0.1230)	343.857 (400.673)
Ramp 3	4.430 (4.3087)	15498.742 (40991.347)	496.672 (519.077)	0.1087 (0.2216)	391.930 (456.689)
Combustor Entrance	2.472	117575.496	1100.464	0.3722	446.724

inlet, larger angles in the cones in the conical configuration are necessary. It is noticeable that a more compressed flow is obtained on the surface of the cones and, as it moves away from the surface, the effects of three-dimensional relief appear.

4.2 Numerical Results

In order to assess the effectiveness of the analytical methodology used, numerical analyzes were carried out seeking solutions for the Navier-Stokes equations for the developed configurations. The inlets were modeled and analyzed using ANSYS – Fluent 19.2 code, Figures 12 and 13 present the defined 2D domain and the main features used for the analysis of each geometry, respectively.

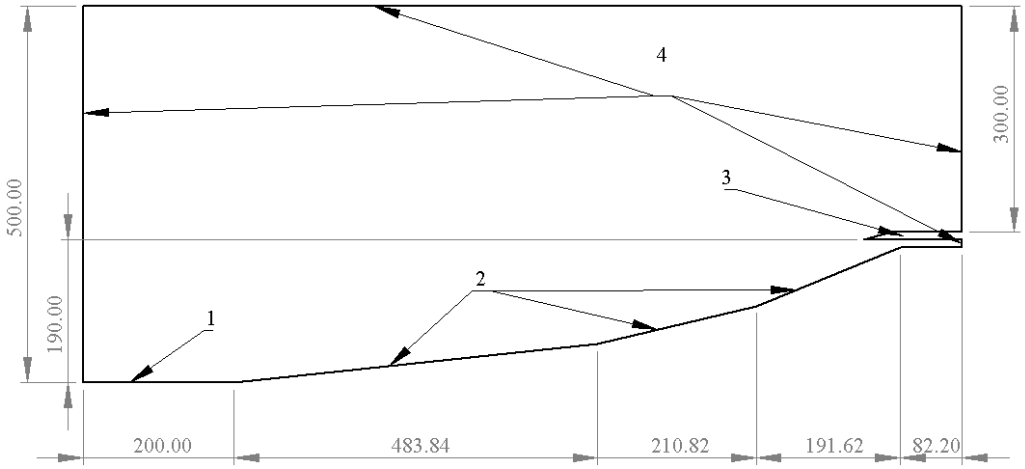

Figure 12: Planar scramjet vehicle dominion.

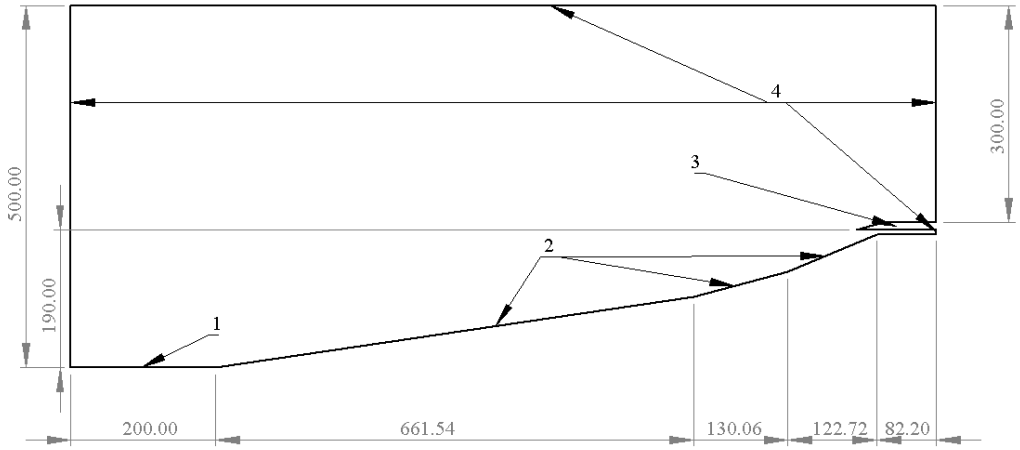

Figure 13: Conical scramjet vehicle dominion.

To nullify the boundary effects, a domain larger than the vehicle dimensions was considered. For this, they were modeled surface 1 and the largest surfaces of region 4 to compose the appropriate domain for the simulation.

Due to the inviscid analysis, a triangular mesh with a maximum element size of 10 mm was considered. In order to generate an adequate mesh, the size of the element on the surfaces of interest and the growth rate of these elements were defined.

For the planar geometry, according to Figure 12, on the surfaces that make up regions 2, an element size wall as defined with 0.75 mm, on the horizontal surfaces of region 3, an element size wall as defined with 0.3 mm and on a slanted surface, 0.2 mm. From the defined surfaces, the size of the elements grows from a rate of 1.0125 until contemplating the entire defined domain, Figure 14.

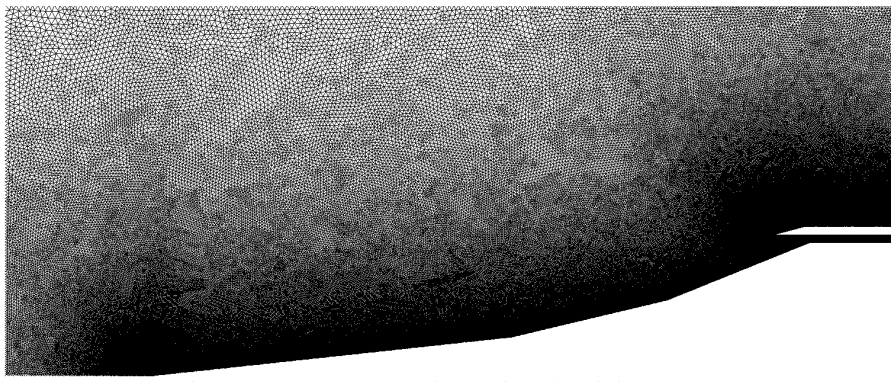

Figure 14: Planar scramjet vehicle dominion mesh.

According to Figure 13, for the conical geometry, the surfaces on region 2, an element size wall as defined with 0.75mm, an element size wall as defined with 0.4 mm and on a slanted surface, 0.3mm. From the defined surfaces, the size of the elements grows from a rate of 1.0125 until contemplating the entire defined domain, Figure 15.

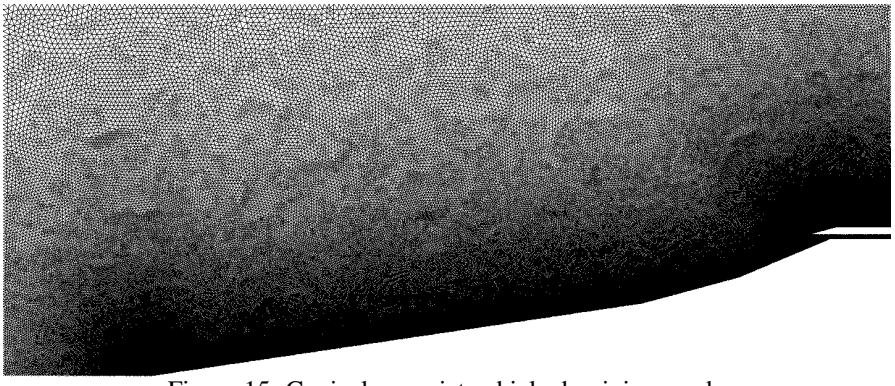

Figure 15: Conical scramjet vehicle dominion mesh.

In planar vehicle analysis setup, planar 2D space and ideal gas were considered. The boundary conditions were defined according to Figure 12. Surface 1 was defined as symmetry, the surfaces at regions 2 and 3 were defined as wall and, the surfaces at region 4 were defined as pressure far field where the ambient and operating conditions of the vehicle were defined.

In the conical vehicle, the same boundary conditions were considered, but, the axisymmetric are defined on 2D space.

In both configurations, it is possible to observe the gradual decrease in Mach number expected when using the total pressure recovery criterion. For the planar geometry, it is considered that the length of the ramps was properly defined to result in on-lip shock and on-corner shock. For the conical geometry, it appears that the approximations considered in the analytical method were adequate and with small variations in the incidence of on-lip shock and on-corner shock. Graphically analyzing the comparison between the analytical and numerical results, Figures 18 to 19, it is verified that, in both cases, there is a convergence between the analytical and numerical methods, demonstrating the effectiveness of the implemented routine.For the conical geometry, it is verified that the small variation in the incidence of on-lip shock and on-corner shock results in the presence of a shock train after the reflected shock wave.

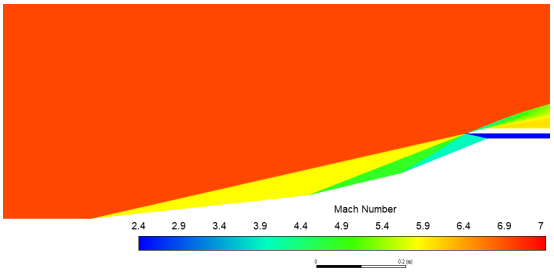

(a) Planar global view in function of Mach number.

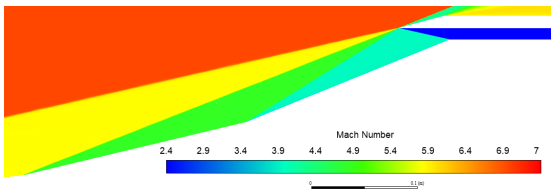

(b) Shock on-lip and on-corner in function of Mach number.

Figure 16: Numerical results for planar geometry.

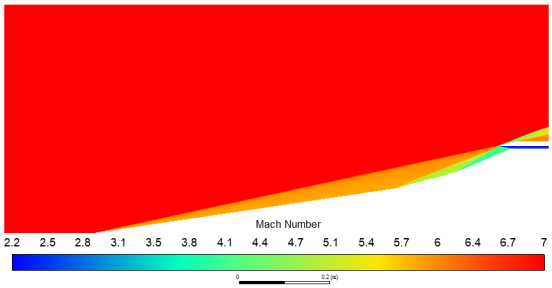

(a) Conical global view in function of Mach number.

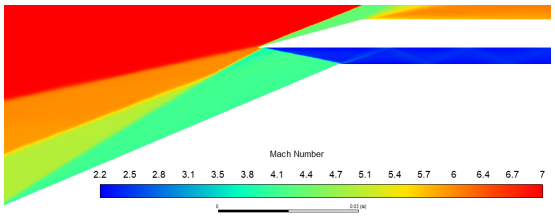

(b) Shock on-lip and on-corner in function of Mach number.

Figure 17: Numerical results for conical geometry.

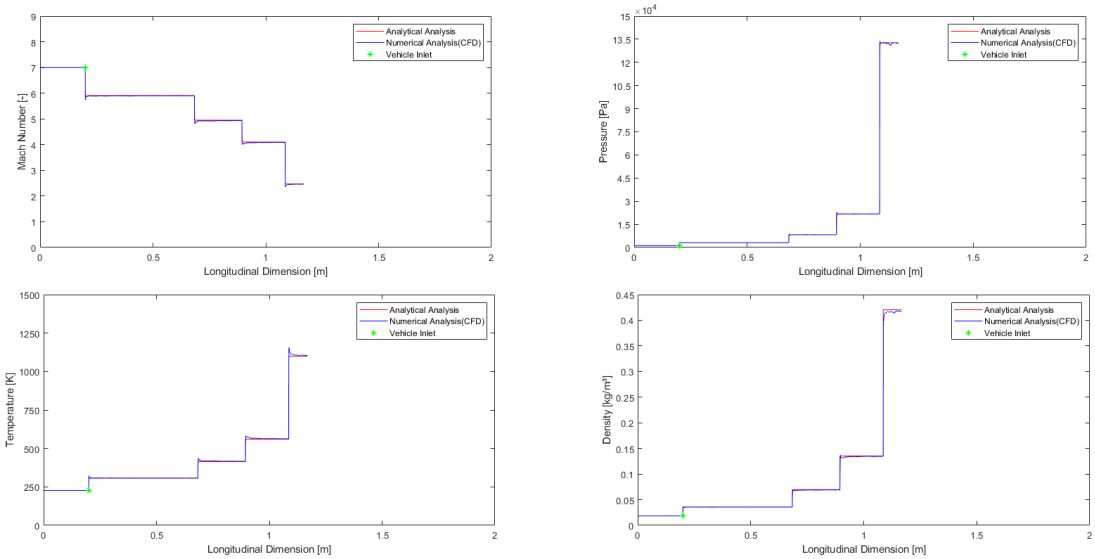

Figure 18: Comparison between analytical and numerical thermodynamic properties for planar geometry.

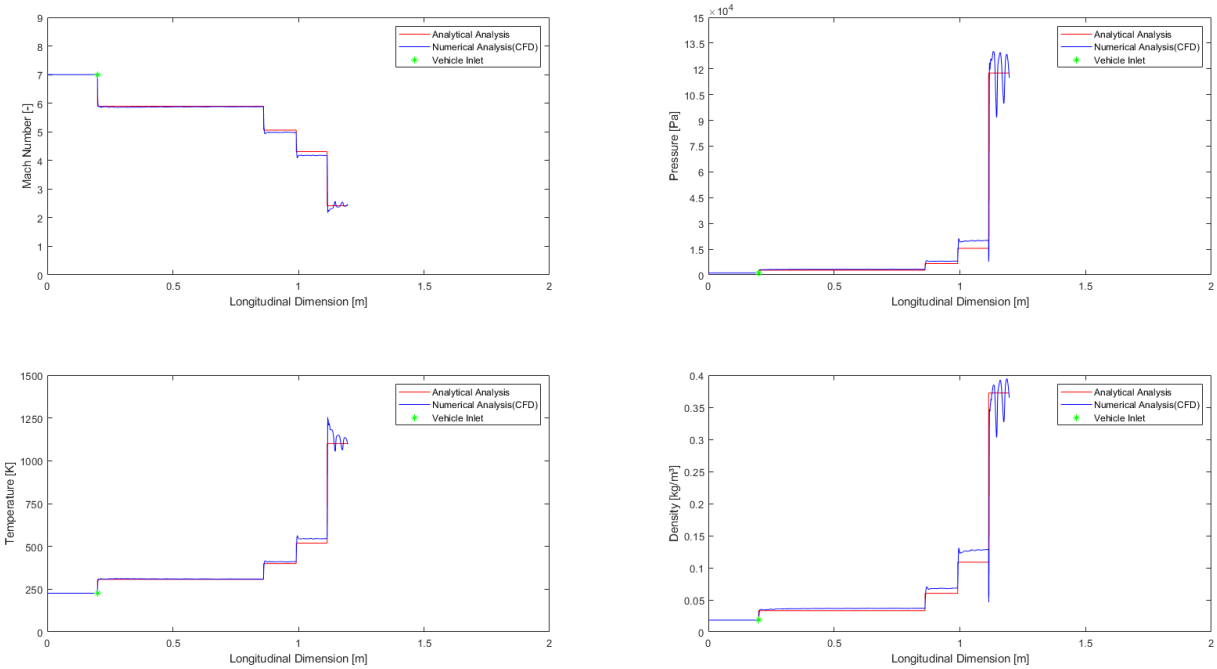

Figure 19: Comparison between analytical and numerical thermodynamic properties for conical geometry.

5. CONCLUSION AND OUTLOOK FOR FUTURE DESIGNS

A methodology for the design of planar and conical inlets of hypersonic airbreathing vehicles was developed using total pressure recovery optimization criteria.

For the planar configuration, the closed relation of the plane oblique shock wave theory was used, which was expanded to a set of ramps. The conical configuration is started from the Taylor-Maccoll solution for conical oblique shock waves and expanded to a set of cones using approaches such as the determination of the flow angle and the mean thermodynamic properties outside the cone surface.

To compare the configurations, a case study was defined in which both had the same design restrictions: Flight at Mach 7, at 30 km of geometric altitude, coupled to a training rocket with known dimensions.

From the results obtained, it was verified that, despite the conical configuration providing a greater mass flow flux on the inlet, cones with larger angles are necessary to perform the same flow compression when compared to the planar configuration. This fact in future analyzes may contribute to greater drag on the vehicle. It was observed that the conical configuration also provides an inlet with a slightly longer length, that is, when considering viscous analysis, the boundary layer can be a considerable factor in choosing the configuration.

By comparing the results obtained in the analytical methodology with the results obtained in the numerical analysis, the convergence between the results was verified. For the conical geometry, due to the different approximations considered, a small variation in the incidence of on-lip shock and on-corner shock was observed, resulting in a shock train after the reflected shock wave.

Finally, the consistency of the methodologies was verified and the importance of comparing analytical and numerical analyzes to obtain concise analysis is highlighted. In addition, factors such as the presence of the boundary layer and real gas considerations must be included in the analysis for the correct choice of a given configuration.

6. ACKNOWLEDGEMENTS

This study was financed in part by the Coordenação de Aperfeiçoamento de Pessoal de Nível Superior - Brasil (CAPES) - Finance Code 001. Also, the authors would like to thank CAPES the support given by the Project PROCAD-DEFESA 88887.626266/2021-00. The authors would like to thank the Instituto Tecnológico de Aeronáutica (ITA), Universidade do Vale do Paraíba (UNIVAP), Universidade Federal do Rio Grande do Norte (UFRN) and a Universidade Federal de Santa Maria (UFSM) to support granted to carry out research on hypersonic airbreathing propulsion.

7. REFERENCES

Anderson, J.D., 2003. *Modern compressible flow: with historical perspective*. McGraw-Hill Education.
Atmosphere, U.S., 1976. *NASA TM-X 74335*.

Curran, E.T. and Murthy, S.N.B., 2000. *Scramjet propulsion*. American Institute of Aeronautics and Astronautics.

Curran, E.T., 2001. "Scramjet engines: the first forty years". *Journal of Propulsion and Power*, Vol. 17, No. 6, pp. 1138–1148.

Heiser, W.H. and Pratt, D.T., 1994. *Hypersonic airbreathing propulsion*. AIAA.

Lassaline, J.V., 2009. "Supersonic right circular cone at zero angle of attack".

Martos, J., 2017. *Aerothermodynamic Design, Manufacture And Testing Of a 3-D Prototyped Scramjet*. Doctor in science in the program of space science and technology, area of space propulsion and hypersonics, Instituto Tecnológico de Aeronáutica, São José dos Campos.

Oswatitsch, K., 1947. "Pressure recovery for missiles with reaction propulsion at high supersonic speeds (the efficiency of shock diffusers)". *NACA Technical Memorandum*, Vol. 1140.

Pereira, M.V.S., 2018. *Projeto Aerodinâmico e Dimensional de um Demonstrador Tecnológico Scramjet Acoplado ao Motor Foguete*. Trabalho de conclusão de curso, Curso de Graduação em Engenharia Mecânica, Universidade Federal do Rio Grande do Norte, Natal.

Pezzella, G. and Viviani, A., 2019. "Introductory chapter: Hypersonic vehicles-past, present, and future insights".

Ran, H. and Mavris, D., 2005. "Preliminary design of a 2d supersonic inlet to maximize total pressure recovery". *AIAA 5th Aviation, Technology, Integration, and Operations Conference (ATIO)*, p. 11.

8. RESPONSIBILITY NOTICE

The authors are the only responsible for the printed material included in this scientific article.

The authors declare that there is no conflict of interest regarding the publication of this scientific article.